A mechanism for sandbar straightening by oblique wave incidence

R. Garnier,[1] A. Falqués,[2] D. Calvete,[2] J. Thiébot,[3] and F. Ribas[2]

Received 22 March 2013; accepted 9 April 2013; published 6 June 2013.

[1] Breaker bars in the surf zone of sandy beaches generally evolve between straight bars parallel to the shore and meandering crescentic bars associated with intense (dangerous) currents flowing seaward through rip channels. Understanding the behavior of such systems is fundamental as they control the entire surf zone dynamics, the shape of the coastline, and the exchange of floating material with the shoreface. Although the mechanisms behind the meandering of an originally straight bar have been studied extensively, a clear physical explanation on the crescentic bar straightening was missing. Recent field observations have highlighted that this morphological reset can be due to wave obliquity. By using a two-dimensional horizontal morphological model, we show that the bar straightening by oblique waves occurs because the rip current is both weakened in intensity and shifted downdrift from the channel deepest section. The technique employed is useful for the study of other types of bed forms. **Citation:** Garnier, R., A. Falqués, D. Calvete, J. Thiébot, and F. Ribas (2013), A mechanism for sandbar straightening by oblique wave incidence, *Geophys. Res. Lett.*, *40*, 2726–2730, doi:10.1002/grl.50464.

1. Introduction

[2] The surf zone of unbounded sandy beaches often exhibits one or several shore-parallel bars where incoming waves predominantly break. Generally, the morphology of a breaker bar perpetually evolves between a configuration where bathymetric contours are almost straight, roughly parallel to the coast, and a situation where the bar meanders with a fascinating regularity [*Short*, 1999; *van Enckevort et al*., 2004; *Price and Ruessink*, 2011, see Figure 1a]. Meandering bars are also known as crescentic bars and are characterized by a sequence of horns and bays due to shallower and deeper sections that break down the uniformity. Typical spacings between two horns are between 100 m and 1 km [*van Enckevort et al.*, 2004]. The breaker bar configuration strongly influences the shoreward morphology of the beach through morphological coupling with an inner breaker bar (if present) [*Castelle et al.*, 2010] or directly acting on the dry beach or through changes in the mean beach profile [*Garnier et al.*, 2008]. Moreover, the plan shape of the breaker bar is coupled to the circulation in the surf zone by conditioning the presence of (dangerous) offshore oriented currents: as waves break in the shallower regions of the crescentic horns, they generate intense (rip) currents often larger than 1 $m\,s^{-1}$ that flow seaward through the deeper sections called rip channels.

[3] The transitions between the straight bar shape and the crescentic shape have traditionally [*Short*, 1999] been associated to the amount of energy of incoming waves: rip channel systems emerge during accretionary conditions (low-energy waves) and, reversely, under erosional conditions (high-energy waves), crescentic bars fast straighten. However, this scheme has been recently revisited by *Price and Ruessink* [2011] and other recent studies (see supporting information for additional references) [*Holman et al*., 2006; *Splinter et al*., 2011] stressing the effect of wave obliquity in the transitions between a straight and a crescentic bar. They find that rip channels seem to develop preferably for normal wave incidence and bar straightening, also called morphological reset, occurs for high oblique waves. Importantly, the bar straightening does not need highly energetic wave conditions.

[4] The mechanisms behind the development of rip channel systems have been studied extensively [*Blondeaux*, 2001; *Dalrymple et al.*, 2011] and it is nowadays well recognized that along unbounded beaches, rip channel systems emerge from the coupling between topography, waves, and currents [*Deigaard et al.*, 1999; *Falqués et al.*, 2000; *Reniers et al.*, 2004; *Calvete et al.*, 2005; *Garnier et al.*, 2008; *Tiessen et al.*, 2011]. However, little attention has been paid to bar straightening probably because numerical models generally predict that rip channel growth accelerates with higher waves [*Calvete et al.*, 2005] rather than decays. Some recent studies (see supporting information) have simulated the morphological reset under oblique wave forcing by attributing it to the increase of alongshore transport but the specific mechanisms are not fully explored. These results are in line with other model studies that already suggested some time ago that rip channel growth is inhibited by oblique waves [*Calvete et al.*, 2005; *Garnier et al.*, 2008]. More recently, *Garnier et al.* [2009] and *Thiébot et al.* [2012] pointed out that oblique waves weaken the instability mechanisms of the origin of the bar meandering due to cross-shore currents.

[5] The present study gives a physical explanation for the recently observed reset of rip channels by oblique waves. A numerical model based on the wave- and depth-averaged shallow water equations (for further details, see *Garnier et al*. [2008]) is used to understand the inhibition of the rip channel formation and the straightening of crescentic bars for uniform stationary moderate energy waves incoming obliquely with respect to the coast.

Additional supporting information may be found in the online version of this article.

[1]Environmental Hydraulics Institute (IH Cantabria), Universidad de Cantabria, Santander, Spain.
[2]Applied Physics Department, Universitat Politècnica de Catalunya, Barcelona, Spain.
[3]LUSAC EA 4253, Université de Caen Basse-Normandie, Cherbourg, France.

Corresponding author: R. Garnier, Environmental Hydraulics Institute (IH Cantabria), Universidad de Cantabria, PCTCAN, C/ Isabel Torres 15, 39011 Santander, Spain. (garnierr@unican.es)

0094-8276/13/10.1002/grl.50464

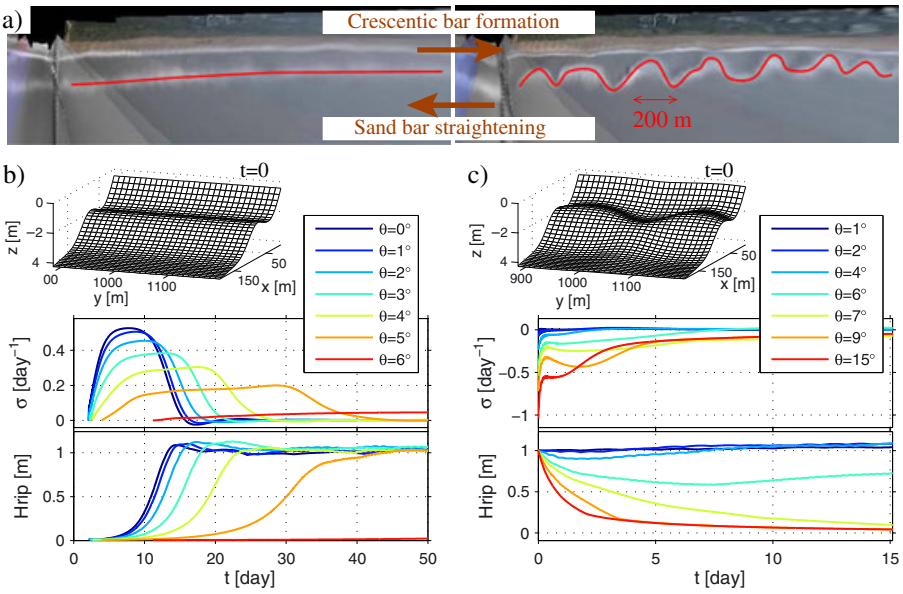

Figure 1. (a) Time exposure images of a straight bar configuration (left) and a crescentic bar configuration (right) of the breaker bar (red lines), Duck, North Carolina, USA. Courtesy of R. Holman, Oregon State University. Numerical experiments: (b) inhibition of crescentic bar formation and (c) sandbar straightening. Time series of instantaneous growth rates of the rip channels σ and of rip channel heights H_{rip}. Colors indicate wave angle θ (see legend). The three-dimensional plots represent the initial bathymetry.

2. Numerical Experiments

2.1. Inhibition of Rip Channel Formation

[6] The formation of rip channel systems over a single-barred beach from self-organization has been tested for different incident wave angles. The initial topography is shown in Figure 1b. It consists of a 250 m wide and 2 km long alongshore uniform beach with a shore parallel bar located at 80 m from the shoreline. At the offshore boundary (D = 4.5m), 1 m waves with a period of 7.5 s are imposed (for more details, refer to *Garnier et al.* [2008]). The incident wave angle at the offshore boundary is constant during the simulations and has been increased from $\theta = 0$ (normal waves) with an increment of 1° for different experiments. The time evolution of the bed level deviation h from the uniform beach is analyzed. At the initial time, h is randomly distributed with an amplitude smaller than 1 cm.

[7] Figure 1b shows the time evolution of the growth rate of the rip channels computed as [*Garnier et al.*, 2006] $\sigma = \frac{\mathrm{d}}{\mathrm{d}t}\left(\frac{1}{2}\|h\|^2\right)/\|h\|^2$, where $\|h\|$ is the norm of the bathymetric perturbation, defined as $\|h\| = \left(\overline{h^2}\right)^{1/2}$, and the overbar indicates the average over the computational domain. Rip channel formation is slower for increasing wave obliquity as the maximum growth rate decreases. However, the rip channel height (H_{rip}, the vertical distance between the shallowest shoal and the deepest channel), is not necessarily smaller for oblique waves and a similar height is observed ($H_{\text{rip}} \simeq 1$ m) for $0 \leq \theta \leq 5°$ (Figure 1b). For $\theta > 6°$ (11° in deep water), the growth rate is so small that the rip channel formation is fully inhibited.

2.2. Bar Straightening

[8] The behavior of an originally well established rip channel system is studied here. The initial state corresponds to the equilibrium state obtained for normal wave incidence, with rip channel systems and associated rip currents (see bathymetry in Figure 1c). Oblique waves have been imposed by first freezing the bathymetry in order to obtain a hydrodynamic equilibrium state (30 min of simulation). The morphological mode is then activated. Experiments have been performed by varying the wave angle from $\theta = 1°$ to 30° ($\theta = 30°$ corresponds to waves incoming almost parallel to the coast in deep water).

[9] At the beginning of the morphological evolution (Figure 1c), the initial growth rate is always negative (i.e., the rip channel height decays at the initial time). For $\theta \leq 6°$, the morphological system rapidly reorganizes so that there is no full destruction but rather a readjustment of the rips. The full reset of the rip channels is observed if the wave angle is greater than 6° that corresponds to the threshold angle from which the self-organization is inhibited. During the reset processes, the height of rip channels fast decreases without any splitting/merging of the rips and the mean beach profile remains unchanged (see supporting information).

3. Physical Mechanisms

3.1. Global Analysis

[10] The exploration of the mechanisms involved in the bar straightening has been performed by means of the so-called "global analysis," which consists of studying the different variables by averaging them over the computational domain (for details, see *Garnier et al.* [2006, 2010] and *Vis-Star et al.* [2008]). In the model of *Garnier et al.* [2008], the sediment transport description is based on the total load formula of *Soulsby* [1997] that can be expressed in the following form: $\mathbf{q} = \alpha\mathbf{v} - \Gamma\nabla h$, where $\mathbf{q}$ is the sediment flux vector, α is the sediment stirring which includes the bed porosity, $\mathbf{v}$ is the current vector, and Γ is the diffusive coefficient depending on α and on the wave orbital velocity at the

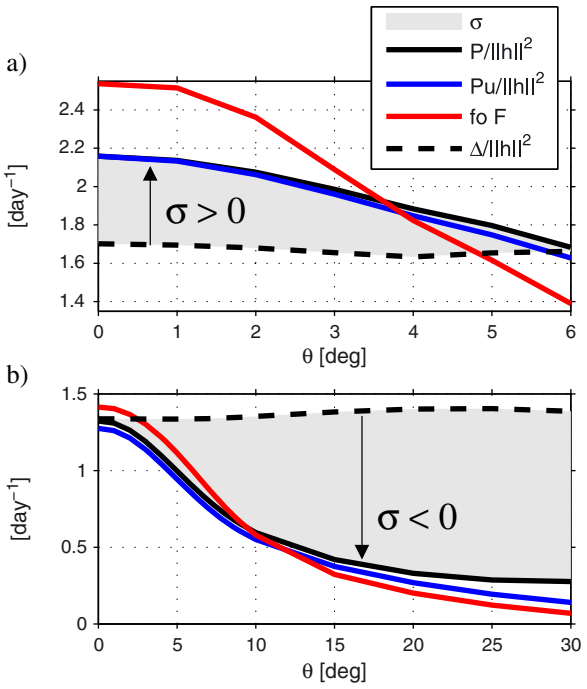

Figure 2. Global analysis. (a) Inhibition of rip channel formation, results computed during the maximum growth. (b) Bar straightening, results computed during the maximum decay. $\mathcal{P}/\|h\|^2$ (black solid line), $\mathcal{P}_u/\|h\|^2$ (blue line), $f_0\mathcal{F}$ (red line), and $\Delta/\|h\|^2$ (black dashed line) as a function of θ. f_0 is a normalizing factor independent of θ(f_0 = $\max_{\theta=0}(D\partial C/\partial x)$ = 4.05 s d^{-1}). The vertical span of the gray patch indicates the growth rate ($\sigma = \mathcal{P}/\|h\|^2 - \Delta/\|h\|^2$).

bottom. For this transport formula, the instantaneous growth rate of the bed forms can be approximated as

$$\sigma = \frac{\mathcal{P} - \Delta}{\|h\|^2}, \qquad (1)$$

where $\mathcal{P}$ and Δ are the production and the damping, respectively, and are defined as $\mathcal{P} = -\overline{hD\mathbf{v}\cdot\nabla C}$, and $\Delta = -\overline{h\nabla\cdot(\Gamma\nabla h)}$, where D is the water depth and $C = \alpha/D$ means a depth-averaged concentration. To understand the mechanisms behind the inhibition of rip channels and the bar straightening, the production and the damping terms ($\mathcal{P}$ and Δ) are analyzed at the time when the maximum growth is obtained during the rip channel formation experiments (Figure 2a) and at the time corresponding to the maximum decay during the bar straightening experiments (i.e., at the initial time, Figure 2b).

[11] The first conclusion shown by Figure 2 is that the unitary damping term $\Delta/\|h\|^2$ is nearly independent of the wave angle. The second conclusion is that $\mathcal{P} \simeq \mathcal{P}_u = -\overline{uhD\partial_x C}$, where u is the cross-shore component of the current. This means that the alongshore component of the current v does not directly contribute to the growth or decay of the rip channels, particularly neither the ambient longshore current nor the feeder currents directly act on the production of rip channels. A further analysis of $\mathcal{P}_u$ by considering that the depth-averaged concentration and the total depth do not depend on the wave obliquity, together with the results shown in Figure 2, shows that the decrease of $\mathcal{P}_u/\|h\|^2$ is due to the quantity $\mathcal{F} = -\overline{uh}/\|h\|^2$, where $\overline{uh}$ is the covariance between u and h. $\mathcal{F}$ can be decomposed by (1) the relative cross-shore current intensity $\|u\|/\|h\|$ and (2) the correlation between the cross-shore component of the velocity and the bed level perturbation $\overline{uh}/\|u\|\|h\|$. Notice that $\mathcal{F} \geq 0$ because seaward currents ($u > 0$) appear in the channels ($h < 0$).

[12] In conclusion, the global analysis allows us to show that both the inhibition of the rip channel formation and the bar straightening by oblique waves are related to the weakening of the production of the instability with increasing wave angle. The production weakening can be due to (1) the decay of the rip intensity for a given bed form or (2) the decreasing correlation between the cross-shore current and the bottom perturbation.

3.2. Rip Current Weakening

[13] The analysis of the rip current systems obtained before starting the bar straightening experiments shows a reduction of the rip intensity, U_{rip} (= max u), as the wave incidence angle increases (see Figures 3 and 4a). Moreover, Figure 4a shows that the ratio between U_{rip} and the channel depth, D_{rip} (= $-\min h$) is the same for well-defined crescentic bars (bar straightening experiments) and for small

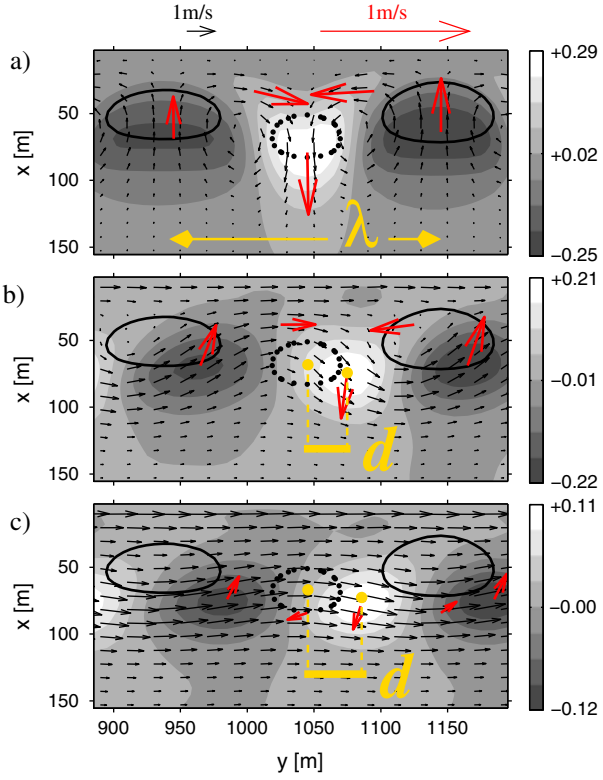

Figure 3. Hydrodynamics over rip channel systems. (a) $\theta = 0$, (b) $\theta = 10°$, and (c) $\theta = 30°$. The coastline is at the top ($x = 0$). Shoals are indicated by solid lines and channels by dotted lines. The gray scale patches represent the cross-shore velocity u (maximum values are rip currents in white) according to the scaling in m/s at the right of the plot. Black arrows represent the total current (u, v). Red arrows represent the residual current ($u, v' = v - V$), where V is the ambient longshore current (V = mean$_y$(v)). λ is the rip channel spacing and d is the rip current alongshore deviation with respect to the central deepest channel section.

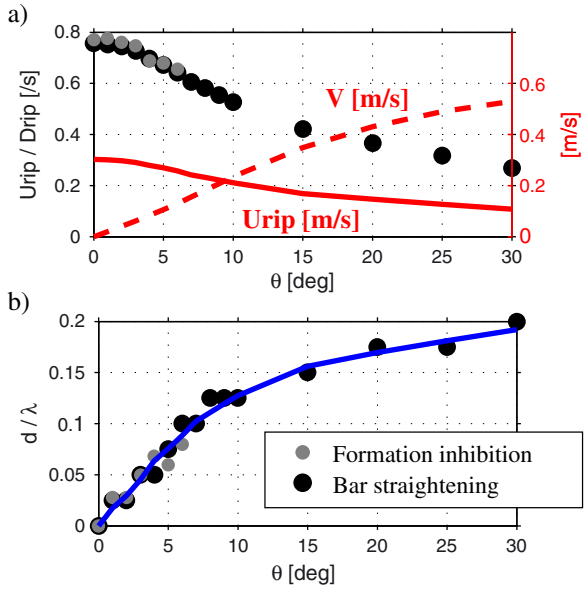

Figure 4. Weakening and shift of the rip current by oblique waves. Gray dots are results of the inhibition of rip channel formation experiments. Black dots are results of the bar straightening experiments. Color lines corresponds to the bar straightening experiments. (a) U_{rip}/D_{rip} as a function of the incident wave angle θ. The red solid line indicates the rip current magnitude U_{rip}. The red dashed line indicates the mean alongshore current over the bar V. (b) A dimensional alongshore shift of the rip current (d/λ) as a function of the incident wave angle θ. The blue line represents approximation (2).

bars obtained during the formation stage (self-organization experiments).

[14] In the present simulations, we see that this reduction of U_{rip} is related to smaller alongshore gradients in wave setup that cause the weakening of the feeder currents turning seaward to flow through the channels with less intensity. For the highest obliquity (for instance $\theta = 30°$) the weakening in wave setup is so strong that the mechanisms leading to the formation of rip currents are different: there are no feeder currents shoreward of the breaker bars (Figure 3c). The rip current is dominated by the variation of the longshore current that is stronger seaward of the bar (larger bottom slope) than seaward of the channels (smaller bottom slope). This alongshore current meandering can be seen as a "current deflection" by the bathymetric features, and the intensity of the rip is thus related to the direction and magnitude of the longshore current. Although there is no field evidence [*Aagaard et al.*, 1997] of the weakening of rip current intensity by oblique waves, this is a general tendency obtained by hydrodynamic numerical models and can be proved theoretically (see supporting information) [*Splinter et al.*, 2011].

3.3. Rip Current Shift

[15] A robust output of those numerical models is the increasing phase lag between u and h with wave obliquity. It is attributed to the effect of the inertia of the longshore current. This phase lag is illustrated in Figure 3 from our hydrodynamic experiments, where the rip current is centered between the two shoals for normal wave incidence (Figure 3a) and is translated by a distance d for oblique waves (Figure 3b,c). An analytical approximation of d can be obtained by using the approximation of *Splinter et al.* [2011], by considering that the mean sea level and the mean wave forcing are in phase with the topographic perturbation, and also by assuming that the feeder currents have the same magnitude as U_{rip} (see supporting information). Thus, d can be approximated as function of the rip spacing λ, the rip current magnitude, and the rip current magnitude that would be observed for normal wave incidence $U_{rip}(\theta = 0)$:

$$\frac{d}{\lambda} \simeq \frac{1}{2\pi}\left[\frac{\pi}{2} - \arcsin\frac{U_{rip}}{U_{rip}(\theta = 0)}\right] \quad (2)$$

A test on this estimate is shown in Figure 4b (compare blue line and black dots). Interestingly, during the rip channel formation experiments, with small amplitude rip channels, the distance d follows the same tendency with respect to θ (compare black dots and gray dots in Figure 4b), so that for small incident wave angles, d increases roughly linearly with θ.

4. Discussion and Conclusions

[16] In order to understand the fundamental mechanisms for bar straightening by oblique waves, highly idealized experiments have been performed based on three main assumptions (see supporting information). First, specific mean (alongshore averaged) initial conditions have been imposed. A different initial bathymetric profile (breaker bar depth, position, double barred beach) or different wave conditions (different wave period or wave height) would give different results and, particularly, a different threshold angle from which the bar is straightened [*Calvete et al.*, 2007]. Second, a specific variability has been imposed in the dynamical system. The offshore wave forcing is assumed to be uniform (time invariant and alongshore uniform). The initial bathymetry has been set with a specific variability. Changes in these variabilities are expected to modify the straightening mechanisms in the same way they can affect the self-organization mechanisms for the rip channel formation [*Reniers et al.*, 2004; *Castelle and Ruessink*, 2011; *Tiessen et al.*, 2011]. Third, the cross-shore transport due to undertow, wave asymmetry/skewness, and boundary layer streaming is assumed to be in balance with the gravitational downslope transport as beach profile changes (due to this cross-shore transport) are slower than the bar straightening processes.

[17] A quantitative comparison with field observations would require very accurate measurements of the bathymetry and of the hydrodynamic forcing conditions, including time and alongshore variability, as shown by the sensitivity of the model results to the initial conditions. Moreover, although the recent observations agree with the mechanism presented here, a clear threshold angle from which the crescentic bars are straightened is difficult to identify. Only *Price and Ruessink* [2011] give a threshold angle that is larger than the one given here. The present study focus on the mechanisms; thus, the results presented (threshold angle) are valid for an idealized situation only. The difference with *Price and Ruessink* [2011] can be explained by the modeling considerations described above (see supporting information).

[18] The basic mechanisms presented here to explain the formation of crescentic bars are related to the so-called "bed-surf" interaction between waves, current, and morphology [*Falqués et al.*, 2000]. The morphological reset by oblique waves is due to the weakening of this interaction leading to a negative feedback between flow and morphology. In his pioneering study, *Sonu* [1968] suggested that nearshore rhythmic patterns arise from interactions between the alongshore current and the bed by analogy with dune formation in rivers (i.e., without waves). From this theory, the rip cells would be due to the deflection of the longshore current over the bed forms, and this so-called "bed-flow" mechanism can be dominant for strong current [*Falqués et al*., 1996]. Here this mechanism does not lead to the formation of rhythmic patterns nor maintain the existing crescentic bars even for the strongest longshore current, but it could be dominant for other conditions.

[19] The bar straightening mechanism can be fully understood from hydrodynamic experiments over fixed rip channel systems. We conclude that crescentic bar straightening by oblique waves occurs because the rip current is both weakened in intensity and shifted downdrift from the channel deepest section to a shallower area. Morphodynamic studies had shown that this alongshore shift causes the migration of crescentic bars [*Deigaard et al*., 1999; *Garnier et al*., 2006]. In the present study, the global analysis has allowed us to demonstrate that it causes, in addition, the straightening of crescentic bars. This technique has been applied to give insight in the fundamental processes in the surf zone, including the dynamics of other surf zone features such as transverse bars [*Garnier et al.*, 2006]; moreover, it has been proven to be useful for the study of other kinds of bed forms [*Vis-Star et al.*, 2008].

[20] **Acknowledgments.** RG acknowledges funding from the Spanish government through the program "Juan de la Cierva." This research is part of the ANIMO (BIA2012-36822) and IMNOBE (CTM2009-11892) projects which are funded by the Spanish government. Thanks to the Coastal Imaging Lab for the use of Argus images. We thank the anonymous referees for their useful comments.

[21] The Editor thanks two anonymous reviewers for their assistance in evaluating this paper.

References

Aagaard, T., B. Greenwood, and J. Nielsen (1997), Mean currents and sediment transport in a rip channel, *Mar. Geol.*, *140*, 25–45.

Blondeaux, P. (2001), Mechanics of coastal forms, *Ann. Rev. Fluid Mech.*, *33*, 339–370.

Calvete, D., N. Dodd, A. Falqués, and S. M. van Leeuwen (2005), Morphological development of rip channel systems: Normal and near normal wave incidence, *J. Geophys. Res.*, *110*, C10006, doi:10.1029/2004JC002803.

Calvete, D., G. Coco, A. Falqués, and N. Dodd (2007), (Un)predictability in rip channel systems, *Geophys. Res. Lett.*, *34*, L05605, doi:10.1029/2006GL028162.

Castelle, B., and B. Ruessink (2011), Modeling formation and subsequent nonlinear evolution of rip channels: Time-varying versus time-invariant wave forcing, *J. Geophys. Res.*, *116*, F04008, doi:10.1029/2011JF001997.

Castelle, B., B. Ruessink, P. Bonneton, V. Marieu, N. Bruneau, and T. Price (2010), Coupling mechanisms in double sandbar systems. Part 1: Patterns and physical explanation, *Earth Surf. Processes Landforms*, *35*, 476–486.

Dalrymple, R., J. MacMahan, A. Reniers, and V. Nelko (2011), Rip currents, *Ann. Rev. Fluid Mech.*, *43*, 551–581.

Deigaard, R., N. Drønen, J. Fredsoe, J. H. Jensen, and M. P. Jørgesen (1999), A morphological stability analysis for a long straight barred coast, *Coastal Eng.*, *36*(3), 171–195.

Falqués, A., A. Montoto, and V. Iranzo (1996), Bed-flow instability of the longshore current, *Cont. Shelf Res.*, *16*(15), 1927–1964.

Falqués, A., G. Coco, and D. A. Huntley (2000), A mechanism for the generation of wave-driven rhythmic patterns in the surf zone, *J. Geophys. Res.*, *105*(C10), 24,071–24,088.

Garnier, R., D. Calvete, A. Falqués, and M. Caballeria (2006), Generation and nonlinear evolution of shore-oblique/transverse sand bars, *J. Fluid Mech.*, *567*, 327–360.

Garnier, R., D. Calvete, A. Falqués, and N. Dodd (2008), Modelling the formation and the long-term behavior of rip channel systems from the deformation of a longshore bar, *J. Geophys. Res.*, *113*, C07053, doi:10.1029/2007JC004632.

Garnier, R., N. Dodd, A. Falqués, and D. Calvete (2009), A mechanism inhibiting rip channel formation for oblique waves, in *Proceedings of Coastal Dynamics,* pp. 1–13, World Scientific, Tokyo, Japan.

Garnier, R., N. Dodd, A. Falqués, and D. Calvete (2010), Mechanisms controlling crescentic bar amplitude, *J. Geophys. Res.*, *115*, F02007, doi:10.1029/2009JF001407.

Holman, R. A., G. Symonds, E. B. Thornton, and R. Ranasinghe (2006), Rip spacing and persistence on an embayed beach, *J. Geophys. Res.*, *111*, C01006, doi:10.1029/2005JC002965.

Price, T., and B. Ruessink (2011), State dynamics of a double sandbar system, *Cont. Shelf Res.*, *31*, 659–674.

Reniers, A. J. H. M., J. A. Roelvink, and E. B. Thornton (2004), Morphodynamic modeling of an embayed beach under wave group forcing, *J. Geophys. Res.*, *109*, C01030, doi:10.1029/2002JC001586.

Short, A. D. (1999), *Handbook of Beach and Shoreface Morphodynamics*, Wiley, Chichester.

Sonu, C. J. (1968), Collective movement of sediment in littoral environment, in *Coastal Eng. 1968*, pp. 373–400, ASCE, London, U.K.

Soulsby, R. L. (1997), *Dynamics of Marine Sands*, Thomas Telford, London, U.K.

Splinter, K., R. Holman, and N. Plant (2011), A behavior-oriented dynamic model for sandbar migration and 2DH evolution, *J. Geophys. Res.*, *116*, C01020, doi:10.1029/2010JC006382.

Thiébot, J., D. Idier, R. Garnier, A. Falqués, and B. Ruessink (2012), The influence of wave direction on the morphological response of a double sandbar system, *Cont. Shelf Res.*, *32*, 71–85.

Tiessen, M., N. Dodd, and R. Garnier (2011), Development of crescentic bars for a periodically perturbed initial bathymetry, *J. Geophys. Res.*, *116*, F04016, doi:10.1029/2011JF002069.

van Enckevort, I. M. J., B. G. Ruessink, G. Coco, K. Suzuki, I. L. Turner, N. G. Plant, and R. A. Holman (2004), Observations of nearshore crescentic sandbars, *J. Geophys. Res.*, *109*, C06028, doi:10.1029/2003JC002214.

Vis-Star, N., H. de Swart, and D. Calvete (2008), Patch behaviour and predictability properties of modelled finite-amplitude sand ridges on the inner shelf, *Nonlin. Processes Geophys.*, *15*, 943–955.